CHEMISTRY
A EUROPEAN JOURNAL

DOI: 10.1002/chem.200500517

VIP

Preparation and Functionalization of Multilayer Fullerenes (Carbon Nano-Onions)

Arno S. Rettenbacher,[a] Bevan Elliott,[a] Joan S. Hudson,[b] Armen Amirkhanian,[a] and Luis Echegoyen*[a]

Abstract: Carbon nano-onions (CNOs) represent a still largely unexplored carbon allotrope. Promising properties of these unique carbon structures are driving the research efforts in this area, but many technical problems remain in their preparation, derivatization, separation and characterization. In this article, we report the preparation, partial purification, and multiple functionalization and solubilization of CNOs. With only one priorly published short communication[1] describing CNO functionalization, the present work is the most comprehensive description of CNO functionalization and characterization to date.

Keywords: carbon · chemical modification · electron microscopy · fullerenes · nanostructures

Introduction

The discovery of fullerenes by Smalley, Curl, and Kroto marks the beginning of the current nanoscience revolution.[2] During the initial stages of fullerene research in the early 90s, two very important and serendipitous discoveries were made, the formation of carbon nanotubes (CNTs) during graphite arc discharge (1991),[3] and the transformation of carbon nanostructures into CNOs under high energy electron beam irradiation during TEM analysis.[4] While CNTs have received and continue to receive a lot of attention due to their many potential applications, the CNO field remains in its infancy. Just as there was a time gap of five years between the discovery of the fullerenes in 1985 and their mass production in 1990, there had not existed a convenient preparation route for CNOs until 2001, nine years after their initial observation in 1992.[3,5]

CNO structures were detected as early as 1980 but remained essentially unnoticed and unexplored until Ugarte observed them upon strong electron beam irradiation of CNTs.[4] This method, however, is impractical to prepare CNOs in large enough quantities for characterization and subsequent development. In the mid 90s other methods were developed to prepare CNOs such as high temperature annealing of nanodiamond particles[6] and implantation of carbon atoms on silver particles.[7] More recently, better synthetic methods have been reported,[8–10] but all of these methods have some limitations and result in relatively low yields of CNOs.

There have been several recent reports, beginning in 1999, targeting the preparation of CNOs containing only a few layers, such as the double-shelled $C_{60}@C_{240}$ and the triple-shelled $C_{60}@C_{240}@C_{540}$.[11] Such structures were prepared in reasonably high yields via laser vaporization of composite carbon–metal targets under low helium pressures and in the presence of C_{60} as a nucleating center.[12] The authors claim to have produced up to 90% yields of these multi-shell fullerenes. Producing CNOs with few layers is desirable to maximize the chance to modify them by chemical reaction, since a smaller-radius particle has a greater surface curvature, and thus, higher chemical reactivity. At the extremes of this reactivity scale are C_{60} and planar graphite, the former exhibiting very rich and varied chemical reactivity and functionalization, while the latter is extremely unreactive and almost inert to chemical derivatization.

Some potential applications of CNOs have been proposed, ranging from optical limiting[13] and catalysis[14] to gas storage.[15] CNOs have also been proposed as possible candidates to account for the 217.5 nm interstellar absorption feature, which, ironically, was the original motivation for the Kroto, Curl, and Smalley experiments in 1985.[16]

[a] Dr. A. S. Rettenbacher, B. Elliott, A. Amirkhanian, Prof. Dr. L. Echegoyen
Department of Chemistry
Clemson University, SC 29634 (USA)
Fax: (+1) 864-656-6613
E-mail: luis@clemson.edu

[b] Dr. J. S. Hudson
Advanced Materials Research Laboratories
91 Technology Dr., Anderson, SC 29625 (USA)

CNOs are also potentially useful in photovoltaic and fuel cell applications. In a very recent article, Kamat et al. electrophoretically deposited single-wall carbon nanotube (SWCNT) films on optically transparent electrodes (OTEs) and measured their photoactivity under excitation by visible light.[17] In an earlier article, the same authors showed that Pt deposited on these SWCNT films possesses a higher catalytic activity for methanol oxidation and oxygen reduction than unsupported Pt on an OTE surface.[18] So it is possible that CNOs, which possess a much larger surface area than single-walled carbon nanotubes (SWNTs),[15] might also be potential candidates for the development of miniaturized fuel cells.

CNOs have also attracted the attention of NASA researchers, who are interested in their tribological properties as additives for aerospace applications.[19] It was demonstrated that these particles can provide adequate and even superior lubrication compared to the commonly used graphitic materials. Very recently, another research group investigated the tribological properties of CNOs in even more detail and concluded that CNOs are indeed superior to conventional lubricants.[20] Here we report the preparation, purification, functionalization and characterization of CNOs using a variety of methods and techniques.

Results and Discussion

For the work described here the synthetic method used for CNO preparation was the arcing of graphite under water, first reported in 2001.[5] As described by Sano et al.,[5] the CNOs formed in an arc between graphite electrodes under water presumably float to the surface of the water due to their hydrophobicity leading to van der Waals crystallites, not because of their density which, at 1.64 $g\,cm^{-3}$, is greater than that of water. However, in our experiments we found that a significant amount of the CNOs could be collected from the bottom of the water vessel after arcing. Comparative transmission electron microscopy (TEM) investigations of the floating (top) and bottom product did not show significant differences in the overall percentage of CNOs found in the samples. Both top and bottom products were found to contain CNOs along with other nanoparticles, such as multiwalled nanotubes (MWNTs) and nanorods (Figure 1). As the overall yield of the CNOs found on the bottom turned out to be about 100-fold greater than the top material, CNOs were collected mostly from the deposit on the bottom.

TEM sample preparation of CNOs usually consists of dipping sample grids into the raw floating CNO product[21] or into the product dispersed in an organic solvent.[1] Since CNOs tend to aggregate in most solvents, even dilute dispersions used for sample collection yield TEM images with very few clearly observable isolated CNOs. Therefore, we employed a method to immobilize the samples in very thin slices (20 nm) of resin in an attempt to obtain clear images of isolated CNOs. Figure 2 shows an HRTEM image of unpurified CNOs generated at 30 A from material obtained from the bottom of the reaction vessel. These CNOs are approximately 20 nm in diameter (30 layers) and clearly show the proper graphitic interlayer distance of 0.33 nm.

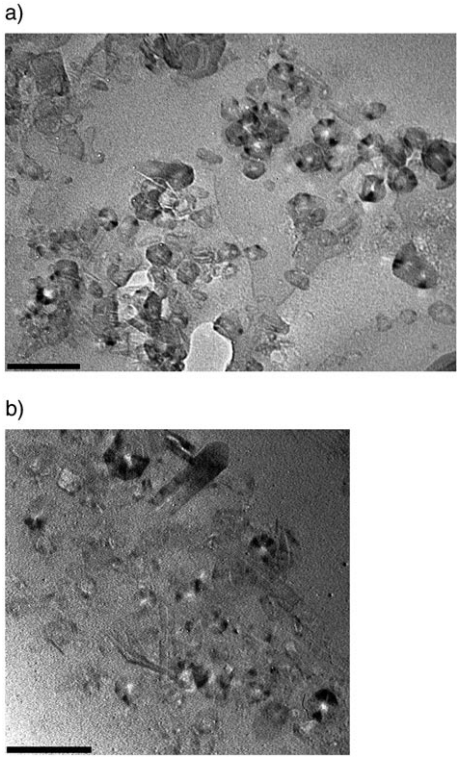

Figure 1. LRTEM (120 keV) image of annealed CNOs from a) top (floating) material and b) bottom material, generated at 30 A (scale bar represents 100 nm).

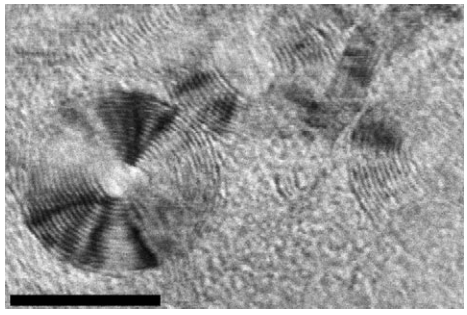

Figure 2. HRTEM image (200 keV) from bottom material, generated at 30 A (scale bar represents 10 nm).

Before attempting any functionalization reactions, these raw CNO samples were partially purified to remove amorphous carbon and graphitic material and to eliminate unwanted side products. The material recovered from the bottom is a mixture of CNOs with amorphous carbon, graphite, nanotubes (SWNTs and MWNTs), nanorods, and other species resembling hollow carbon nanospheres. The largest pieces of graphite were removed by hand with tweezers, and all the remaining amorphous carbon was eliminated

by annealing the samples in air. TGA experiments were first performed in order to find optimal annealing conditions, and all subsequent annealings were carried out for 1 h at 400 °C. Depending on the specific experimental conditions used for carbon onion generation, the weight loss after elimination of the amorphous carbon was approximately 10–30 %.

Further purification consisted of sample treatment with nitric acid between 3 and 11 M followed by thermal annealing or microwave heating. Optimization of the purification steps was monitored by TEM. Under convective heating, optimal purification was obtained by refluxing for 48 h with dilute nitric acid (3 M). In the case of microwave heating in HNO_3, 70 % HNO_3 yielded cleaner CNO samples within 30 min. Figure 3 shows representative TEM images of the

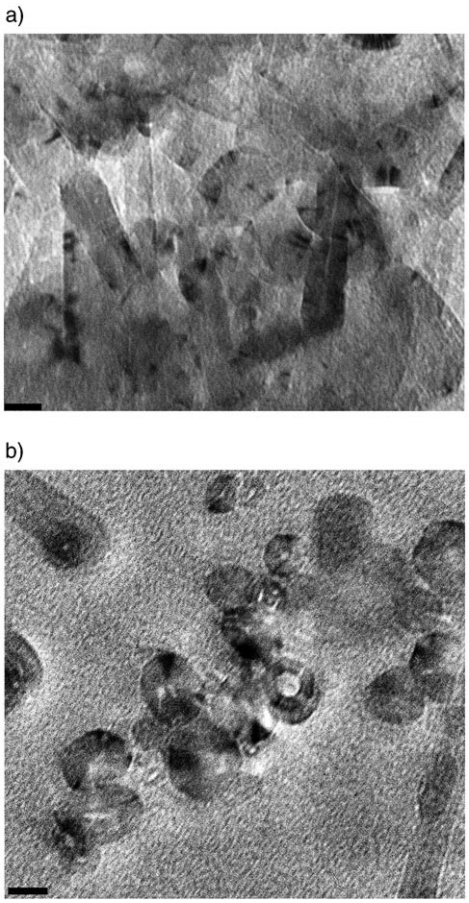

Figure 3. LRTEM (120 keV) image of a) unpurified (30 A) and b) purified (annealing, HNO_3/microwave) CNOs (30 A, scale bar represents 20 nm).

CNOs before and after the annealing/HNO_3/microwave treatment purification procedure. The purification steps involving nitric acid have been shown to form carboxyl functionalities on the surface of CNTs.[22–24] These should facilitate further functionalization for CNOs as well.

Treatment with supercritical water (SCW) was also investigated, but only preliminary results are in hand. Only one experiment has been completed so far, but the TEM images suggest that even smaller CNOs are obtained after SCW treatment as can be seen in Figure 4. Further work is currently underway using SCW to purify CNOs in our laboratories.

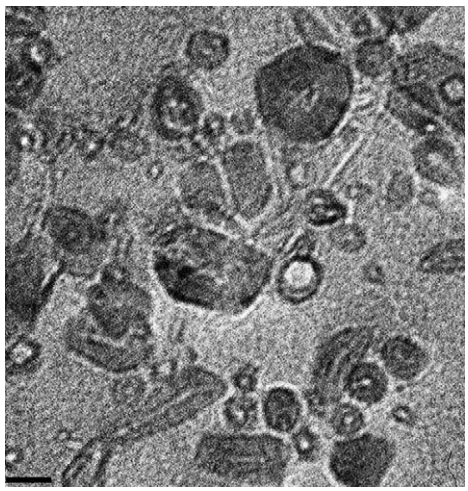

Figure 4. Purified (annealing, HNO_3/microwave, SCW, annealing) CNOs (30 A). Scale bar represents 20 nm.

Organic Functionalization of CNOs

CNOs are totally insoluble in organic and inorganic solvents, similar to single-walled carbon nanotubes (SWNTs). This lack of solubility hinders the study of their chemical and physical properties. So far, the only organic functionalized and solubilized CNOs were reported by Prato and co-workers.[1] They claimed to have prepared solubilized CNOs but the characterization reported, based on TEM, was somewhat unclear. In addition, their starting material did not contain large percentages of CNOs.

Though CNOs are different in morphology than SWNTs, they are similar enough to warrant attempts to use the same reactions as those commonly employed with SWNTs. So far, two different approaches have been developed for derivatizing SWNTs: direct sidewall addition and functionalization at defect sites. Typically, the latter takes advantage of the carboxylic acid moieties at the defect sites to link polymeric and oligomeric functional groups. There is already strong experimental evidence for the existence of nanotube-bound carboxylic acids and also evidence showing that reactions targeting the carboxylic acids result in the solubilization of the nanotubes. For further successful reactions with amino-terminated compounds, the presence of those carboxyl groups is very crucial. A considerable difference between nanotubes and CNOs is of course the fact that the latter do not have easy accessible open ends, which facilitate oxidation.

Herein, two successful reactions are described, both of them utilizing free available carboxyl groups, and a third describes the already reported azomethine ylide addition reaction (1,3-dipolar cycloaddition reaction).[1]

Preparation of water soluble CNOs with diamine-terminated oligomeric poly(ethylene glycol) (Scheme 1): To our knowledge, this is the first report of water-soluble CNOs. Three different types of reactions with carbon onion-bound carboxylic acids should be possible: direct acid–base interaction, amidation via the in situ generated acid chloride, and carbodiimide-activated coupling. Each of these approaches have been successfully reported for SWNTs,[25] and the most simple type, direct amidation, seems to yield the best results. Therefore, we used similar conditions to those reported for the successful direct functionalization and solubilization of single walled carbon nanotubes by diamine-terminated PEG compounds.[25] Longer reaction times (up to 6 d) and higher reaction temperatures (up to 140 °C) gave higher yields, so we reacted the CNOs at the same maximum temperature but for longer times.

A low resolution TEM image (Figure 5a) of the unpurified reaction product which was completely soluble in water, showed the presence of CNOs, but was dominated by other, unidentifiable byproducts. Those side products were removed by dialysis and a LRTEM of the remaining black powder revealed a higher concentration of CNOs (Figure 5b).

Strong evidence for the presence of CNOs in the soluble samples is also provided by thermal defunctionalization results. The defunctionalization (under inert gas) is based on the fact that the temperature required for the evaporation of the carbon onion-bound functional groups (PEG_{1500N}) is considerably lower than that of the CNOs, enabling the selective removal of the functional groups in a thermal gravimetric analysis (TGA) scan. Figure 6 shows that after the TGA experiment, 18% of the starting material remained. Since TEM cannot probe the result of this defunctionalization, a Raman spectrum of the PEG-derivatized CNOs before and after the TGA experiment revealed the success of the derivatization process as well as of the subsequent thermal defunctionalization. Figure 7 clearly shows that after heating, all PEG groups were eliminated. Since only defect functionalization was carried out and no additional defects should have been introduced to the CNO cage, theoretically there should be no pronounced difference between the Raman spectra of the starting material (Figure 7, bottom) and the PEGylated form (Figure 7, middle). However, the PEGylated CNO sample yields a broad continuum in contrast to the visible discrete peaks from the unfunctionalized CNOs. The same effect can be seen in Raman spectra of PEGylated nanotubes.[25] This spectral difference is due to the strong background fluorescence of the long PEG chains which dominate the much weaker Raman bands of the CNO cage.

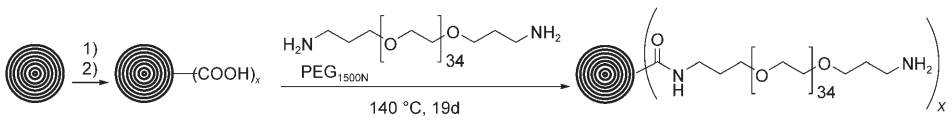

Scheme 1. PEGylation of CNOs: 1) 1 h, 400 °C; 2) refluxing in 3 M HNO_3 for 48 h.

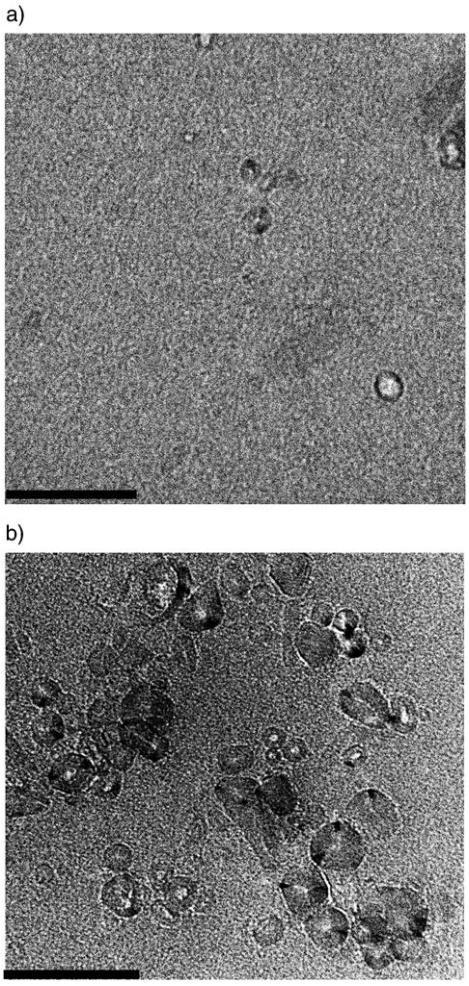

Figure 5. LRTEM (120 keV) image of water soluble, PEG-derivatized CNOs a) before and b) after 300 kD dialysis (scale bar represents 100 nm).

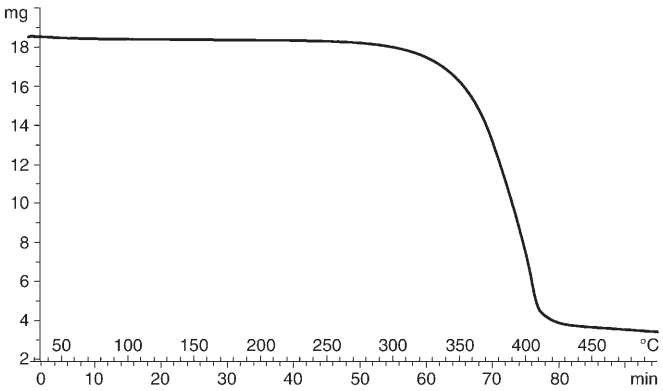

Figure 6. TGA of PEG-derivatized CNOs (18.5 mg, 5 °C min^{-1}, N_2 50 mL min^{-1}).

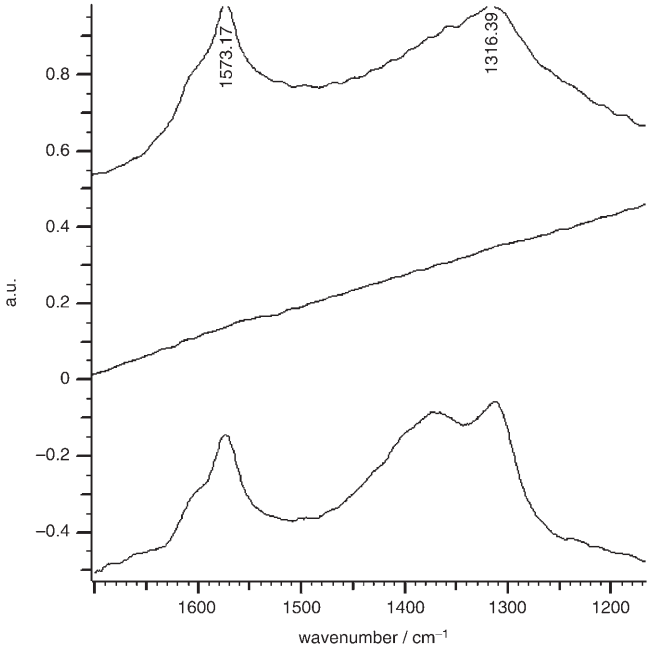

Figure 7. Raman of defunctionalized CNOs after TGA (top), PEG-derivatized CNOs (middle) and CNOs as starting material before derivatization (bottom).

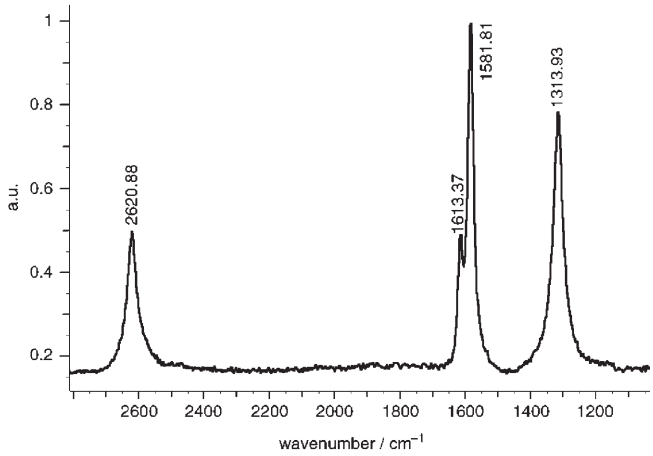

Figure 8. Raman spectra of CNO thin film (starting material, 30 A, electrophoretically deposited on ITO electrodes).

The Raman spectrum at the top of Figure 7 exhibits *D* and *G* bands typical for CNOs.[21,26] The broad band at about 1580 cm^{-1} corresponds to the E_{2g} mode in the graphite structure of carbon. In the spectral range from 1200 to 1700 cm^{-1}, ideal single-crystal graphite shows only this band at 1580 cm^{-1}.[27] In addition to the *G* band, the *D* band appears at about 1320 cm^{-1} for finite-size crystals of graphite (e.g., polycrystalline graphite).[28,29] Speculation about the true origin of this band exists.[30,31] The width of the *G* band is related to the disorder within the carbon sp^2 sheets.[28] To our knowledge, Raman spectra of CNOs reported in the literature typically exhibit broad features, as shown in Figure 7, with one exception.[16] To investigate the 217.5 nm feature of the interstellar spectrum in 2003,[16] Sano and coworkers produced CNO thin films on quartz disks for UV spectra. The Raman spectra of the same quartz disks showed a very sharp *G* band after annealing, indicating the presence of a highly ordered nanocrystalline graphitic material.

The above results encouraged us to obtain Raman spectra of various compounds that were electrophoretically deposited on ITO electrodes. Figure 8 shows interesting results. The *G* band at 1582 cm^{-1} was sharp enough to allow the observation of another band at 1613 cm^{-1}. This band has been described as a shoulder (as in Figure 7) of the dominating *G* band.[21] It is assigned as a *D′* peak and is also a disorder-induced peak[32] and thus not observed in highly orientated pyrolytical graphite (HOPG), but often observed in highly defective graphite. The Raman spectra in Figures 7 and 8 are from the same material (CNOs produced at 30 A), and were obtained under the same conditions and parameters. Noteworthy also is the strong and sharp band at 2621 cm^{-1}, which is normally barely visible. This observation has been made before by Sano et al.[16] after annealing of their carbon onion thin films deposited on quartz disks. Before the annealing process, this peak was hard to see, but afterwards, it became very strong and relatively sharp. This sharp and intense band is attributed to the presence of highly ordered graphitic materials such as the CNOs. It is virtually absent in amorphous carbon and graphite.[19,33]

A comparative study of the ^{1}H NMR spectra of the starting material PEG_{1500N} and the PEGylated CNOs in $CDCl_3$ shows small but significant differences (Figure 9). In both spectra the very intense multiplet at 3.53 ppm for PEG_{1500N} and 3.62 ppm for PEGylated CNOs dominates the spectrum as expected, since this strong signal corresponds to the 68 CH_2 groups vicinal to two O atoms. However, the two weak broad signals at 2.28 and 2.68 ppm (the six terminal CH_2 groups) in the ^{1}H NMR for the starting material disappear completely in the ^{1}H NMR for the PEGylated CNOs. The absence of signals from the terminal CH_2 groups suggests a successful derivatization of the carboxylated CNOs, at both of the terminal NH_2 groups of the long PEG chain. The closer the protons or carbon atoms of the PEG chain are to the outer shell of the CNO, the more likely they will experience different chemical environments due to the presence of CNOs of different sizes and to the close proximity to other PEG chains. Therefore, the signals from these nonequivalent nuclei do not add up to one strong signal, but are each too weak to be observed.

A comparative study of the ^{13}C NMR spectra (Figure 10) yields clearer results and shows similar behavior. Some chain carbon signals disappear completely in the functionalized CNO sample, while others remain visible and unshifted. The three strong signals at 33.2 (C-2, where the number refers to the relative position from the terminal hetero element N), 39.5 (C-1) and 69.4 (C-3) ppm in the PEG_{1500N} starting material spectrum disappear in the PEGylated CNO spectrum. This again suggests that the signals from at least the three carbon atoms (C-1, C-2, C-3) closest to the

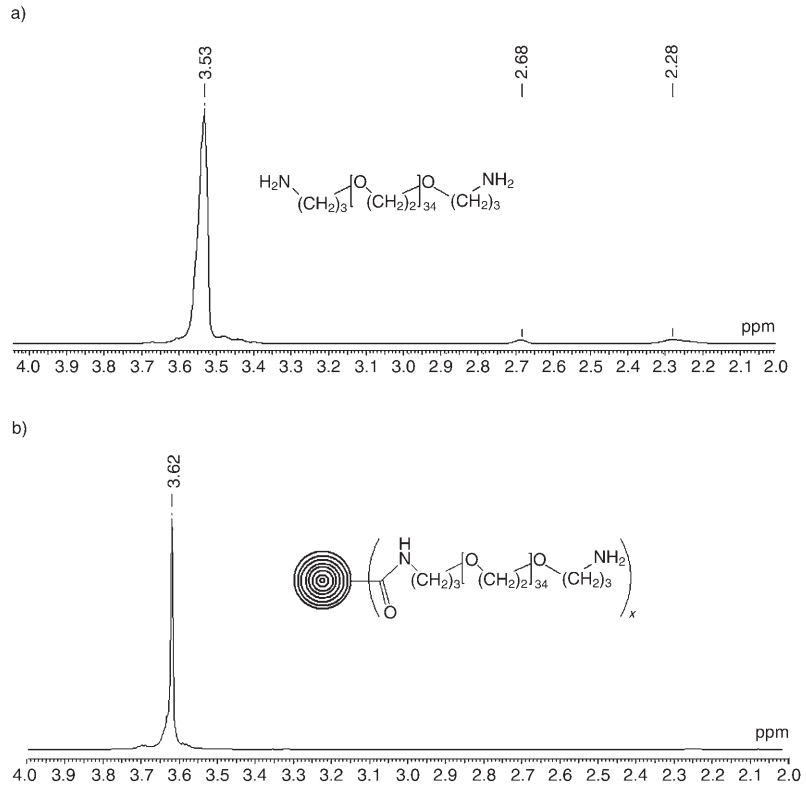

Figure 9. ^{1}H NMR (500 MHz, $CDCl_3$) of a) starting material PEG_{1500N} and b) PEGylated CNOs.

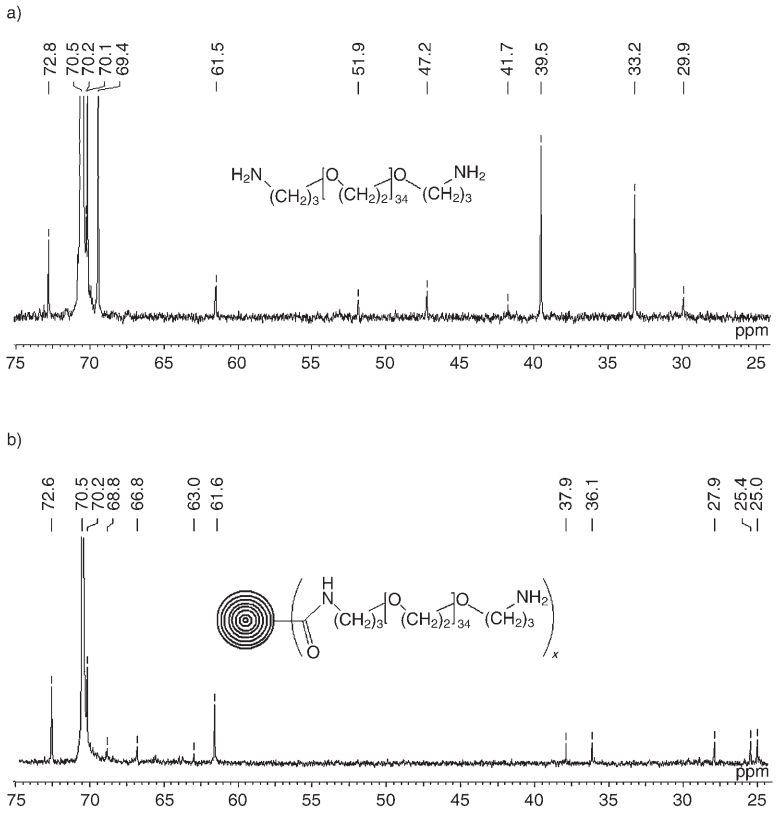

Figure 10. ^{13}C NMR (500 MHz, $CDCl_3$) of a) starting material PEG_{1500N} and b) PEGylated CNOs.

CNO cage are broadened beyond observation for the same reasons already mentioned before.

In a recent article[39] as well as in the references cited therein, the authors discussed the fact that ^{1}H and ^{13}C NMR spectra of monolayer-protected gold clusters (MPCs), compared with those of unbound ligands, display resonances that are substantially line-broadened. For hexanethiolate and related ligands they showed this broadening effect to be lowest for terminal nuclei and highest for nuclei closest to the gold core. In another article,[40] ^{1}H NMR spectra for two different sized phenylethanthiol-derivatized gold clusters, one consisting of 38 Au atoms with an average diameter of 1.1 nm and one consisting of 140 Au atoms with an average diameter of 1.6 nm, were compared. The authors showed that the smaller derivatized cluster Au_{38}-$(PhC_2S)_{24}$ MPC exhibits resonances nearly as sharp as those of the free ligand 2-phenylethanthiol, whereas the larger Au_{140} nanoparticle shows very broad and featureless peaks. An extrapolation of this gold nanoparticle size effect to our larger carbon nanostructures seems justified. Since the CNOs in this study have an average diameter of about 20 nm, it is not surprising that the resonances for the ^{1}H and ^{13}C nuclei closest to the CNO cages are not detectable.

The reasons for this extreme line broadening, leading to the disappearance of the signals, have been discussed extensively elsewhere[41–43] for the case of alkanethiolate monolayers on gold clusters. Since the alkyl chain-functionalized CNOs are analogous, these previously delineated line broadening arguments can be applied in the current study: 1) the tight packing of protons close to the CNO

cage causes rapid spin–spin relaxation from dipolar interactions; 2) there are different chemical shifts for ligands attached at different carboxy binding sites on the CNO outer cage surface; 3) the chemical shift differences vary with CNO size and structure, and 4) longer correlation times of the nuclei closest to the large CNO surfaces can lead to shorter relaxation times and consequent broadening.

The very large number of carbon atoms in the outer shell of different-sized CNOs makes their individual detection by carbon NMR unlikely. Separate 48-hour ^{13}C NMR experiments of the PEG_{1500N} starting material and the PEGylated CNOs have been run. While the starting material shows no peaks, the functionalized CNO sample shows a broad signal in the aromatic carbon region with a maximum intensity around 115 ppm, indicative of surface carbons on the CNOs. As a comparison, C_{60} shows a single peak at 142.7 ppm.

Preparation of soluble CNOs with oligomeric alkyl amide functionalities (Scheme 2): 1-Octadecylamine (ODA) has been described in the literature in recent years as a very good agent for the amidation of the terminal carboxylic groups in nanotubes.[34–37]

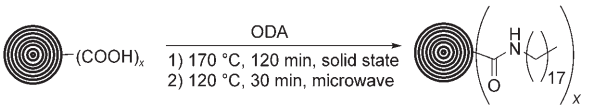

Scheme 2. Synthesis of ODA-derivatized CNOs.

Solid-state reaction: To perform the amide derivatization with the CNOs, we employed the procedure reported for MWNTs by Basiuk et al.,[38] a solid-state reaction between purified CNOs and ODA. After workup, a stable and transparent green solution in $CHCl_3$ was obtained and a drop was placed onto a copper grid for TEM analysis. A representative TEM image can be seen in Figure 11. Significant amounts of soluble CNOs with diameters from 5 to 25 nm can be seen, together with some large nanorods. The Raman spectrum looked very similar to the one shown for the PEGylated CNOs in Figure 7 (middle). The weight gain due to the octadecyl chains was 39% after derivatization.

We also observed covalently linked octadecyl groups on the CNO surface by NMR. To show that the solubilized CNOs were really chemically functionalized and not a mixture of ODA and CNOs, we performed ^{1}H and ^{13}C NMR experiments of starting material and functionalized CNOs under the same conditions and compared the resulting spectra. Figure 12a shows a 500 MHz ^{1}H spectrum of starting material ODA, and Figure 12b a similar spectrum from the ODA-derivatized CNOs. The triplet at 2.65 ppm (CH_2-1) disappears in the derivatized CNO spectrum, as does the multiplet at 1.40 ppm (CH_2-2). The broad signal around 1.6 ppm in Figure 12b is due to HOD since addition of D_2O shifted the

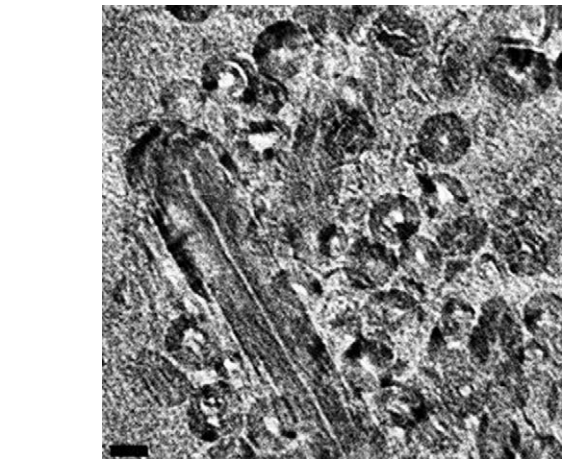

Figure 11. LRTEM (120 keV) of ODA-derivatized CNOs from solid-state reaction (bar represents 20 nm).

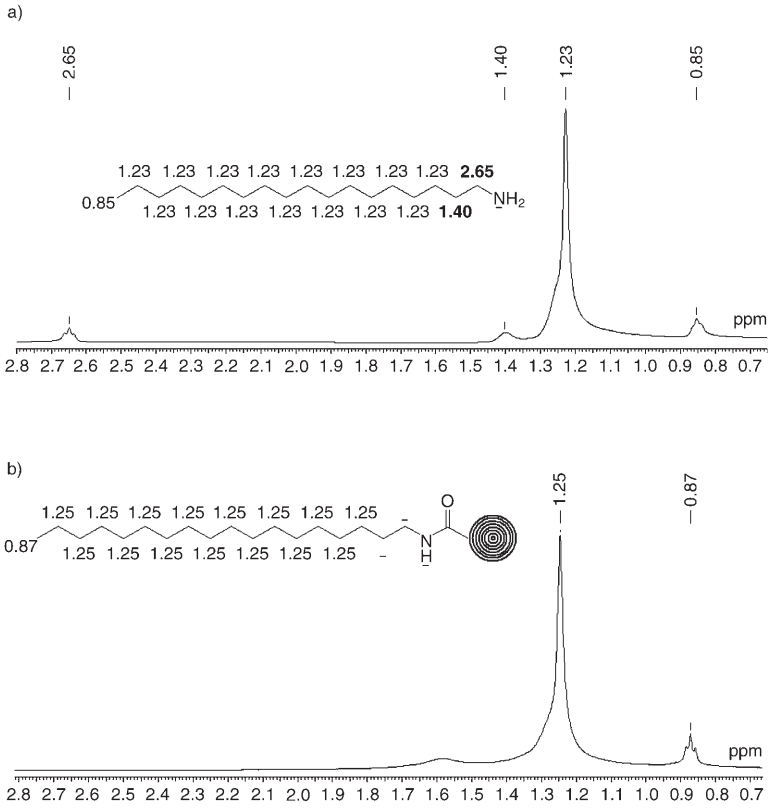

Figure 12. ^{1}H NMR (500 MHz, $CDCl_3$) of a) starting material octadecylamine (ODA) and b) ODA-derivatized CNOs; insets show structures with simulated chemical shift assignments.

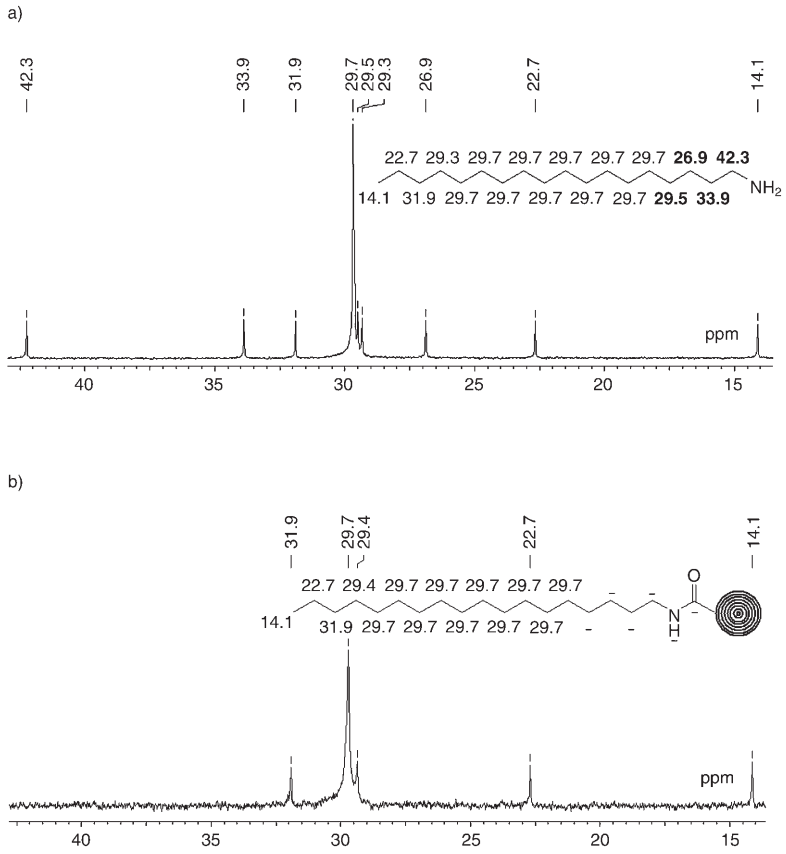

Figure 13. ^{13}C NMR (125 MHz, $CDCl_3$) of a) starting material ODA and b) ODA-derivatized CNOs; insets show structures with simulated chemical shift assignments.

signal. (HOD does not appear in Figure 12a due to a higher concentration of the ODA.) The signals from the CH_3 group at 0.85 ppm (0.87 ppm in case of the ODA-derivatized CNOs) and the CH_2 groups at 1.23/1.24 ppm did not disappear, because these are farther away from the carbon onion surface. Even more compelling is the comparative ^{13}C NMR spectrum (Figure 13). The four closest carbon atoms at 42.3 (C-1), 33.9 (C-2), 26.9 (C-3) and 29.5 ppm (C-4) disappear completely in the derivatized CNO spectrum.

The very large number of carbon atoms in the outer shell of different-sized CNOs makes their individual detection by carbon NMR unlikely. After running a saturated sample of ODA-derivatized CNOs for 48 h, a significant rise of the background in the expected aromatic carbon region was visible (maximum at ca. 115 ppm). A similar experiment with an ODA solution under the same conditions showed no aromatic carbon signal. Therefore, it is probable that this broad signal arises from the collection of nonequivalent carbons in the nano-onions' outer cages.

Microwave reaction: Motivated by a recent article[44] where the microwave-induced rapid chemical functionalization of single-walled carbon nanotubes utilizing 2,6-dinitroaniline was described, a suspension of purified CNOs and ODA in dimethylformamide (DMF) was submitted to microwave irradiation. After workup, an insoluble black residue and a soluble part were obtained. To prove the presence of CNOs in the soluble fraction, one drop of a very dilute $CHCl_3$ solution was placed onto a copper TEM grid. A representative TEM image can be seen in Figure 14. The weight gain due to derivatization in the case of the microwave approach was slightly better (42 % compared with 39 % for the solid-state reaction). The Raman spectrum of this product also showed no characteristic features. Comparing the results from the microwave reaction with the solid-state reaction by TEM, the latter reaction yield is slightly less, but is qualitatively similar in all other respects. NMR investigations (^1H and ^{13}C) of this sample showed exactly the same results as discussed previously for the case of ODA-derivatized CNOs obtained by the solid-state reaction.

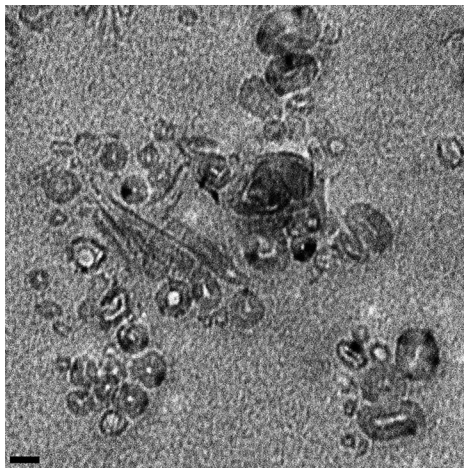

Figure 14. LRTEM image (120 keV) of ODA-derivatized CNOs from microwave reaction (bar represents 20 nm).

Preparation of soluble CNOs by 1,3-dipolar cycloaddition (Scheme 3): This functionalization methodology is based on the 1,3-dipolar cycloaddition of azomethine ylides generated by condensation of an α-amino acid and an aldehyde, a reaction that Prato and co-workers have widely applied to the organic modification of fullerene C_{60}.[45,46] The same research group has successfully applied this reaction on SWNTs[47]

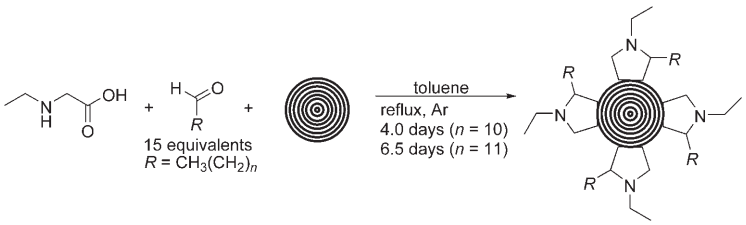

Scheme 3. Synthesis of pyrrolidine-derivatized CNOs.

and in a more recent article,[1] to solubilize CNOs. The solubilized CNOs described had diameters between 60 and 300 nm, whereas our functionalized CNOs have diameters between 5 and 25 nm. The article described the space between the internal shells as having a mean value of about 4 nm, which does not correspond to graphitic materials. It is well established in the literature[5,21] that CNOs have about the same interlayer distance between successive concentric spheres as graphite, that is 0.33 nm. HRTEM images of our derivatized CNOs show the same distance. The carbon onion shown in Figure 15 has 32 shells, and a radius of

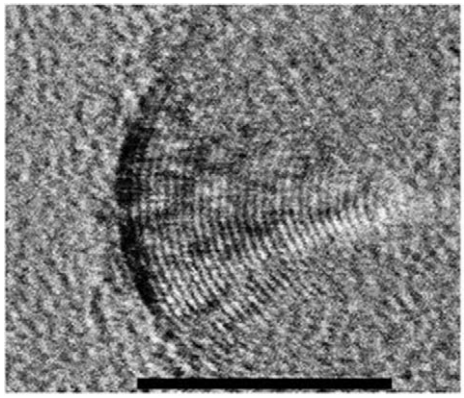

Figure 15. HRTEM image (200 keV) of pyrrolidine-derivatized CNOs (scale bar represents 10 nm).

10.5 nm. A simple calculation of the inter-shell distance yields a mean value of 0.33 nm. Therefore, the solubilized CNOs reported here conform to the expected interlayer distance and structural properties for these materials.

A more representative image of the whole sample can be seen in Figure 16a. Many differently-sized CNOs are present, along with nanorods that have also been derivatized. It is one of our future goals to separate CNOs from nanorods and to separate CNOs based on size.

To improve solubility, an alkyl chain can be attached to the outer shells of the CNOs. As the azomethine ylide reaction needs an amino acid and an aldehyde to generate the 1,3-dipolar species for the cycloaddition, it is in principle possible to introduce the alkyl chain via the aldehyde or the amino acid. Prato et al.[1] used paraformaldehyde and 2-(2-(2-(2-methoxyethoxy)ethoxy)ethylamino)acetic acid to introduce a long chain. In the present work, the long chain was introduced via the aldehyde because of easier accessibility.

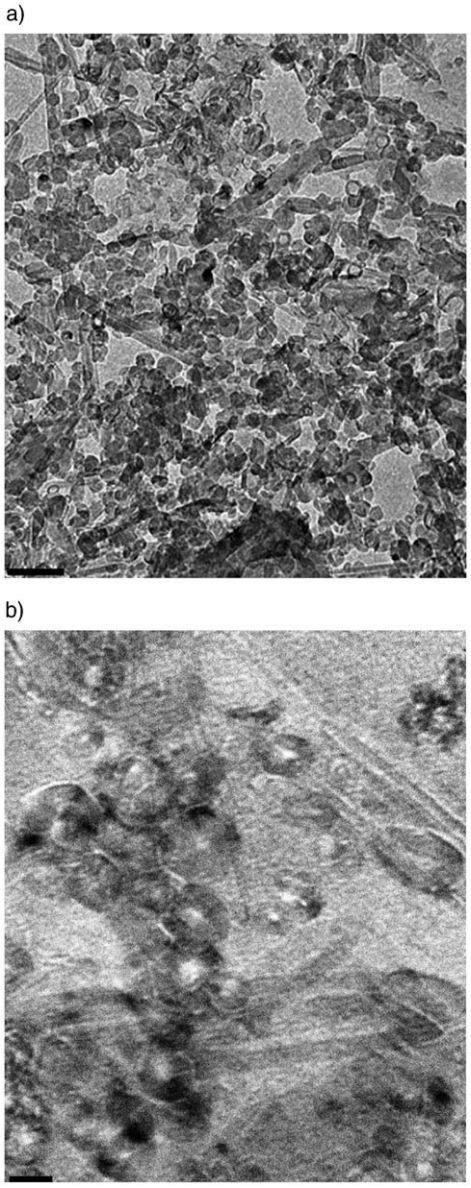

Figure 16. LRTEM image (120 keV) of pyrrolidine-derivatized CNOs, a) R = $CH_3(CH_2)_{10}$ (scale bar represents 100 nm) and b) R = $CH_3(CH_2)_{11}$ (scale bar represents 20 nm).

After workup, *solution 1*, solution *3*, and *solids 1–3* were checked for CNOs by TEM (Figure 17). TEM investigation of *solid 2* and *solid 3* showed no difference: both samples consisted of CNOs. This result is in contrast to that reported, where "carbon onions" were found only in the soluble part and amorphous carbon in the insoluble part.[1]

As TEM is only an indicator to show the presence or absence of CNOs, and can never differentiate between derivatized and nonderivatized CNOs, this result simply shows that *solid 2* consists of a mixture of unreacted and partially derivatized CNOs. Further refluxing of *solid 3* with the amino acid and the aldehyde as described above should afford additional soluble CNOs. Replacing thermal heating with microwave irradiation could facilitate the cycloaddition and lead to better yields in a shorter amount of time.

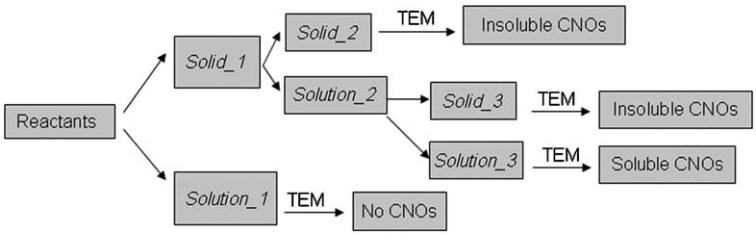

Figure 17. Synthesis of pyrrolidine-derivatized CNOs.

Replacing the lauraldehyde with the homologous aldehyde tridecanal leads to higher yields: a weight gain of 47% and therefore a much higher functionalization of the pristine CNOs was obtained. A TEM image of *solution 3* (Figure 17) shows the presence of CNOs in the size range of about 10 to 25 nm (Figure 16b).

In order to obtain Raman spectra of good quality, the pyrrolidine-derivatized CNOs were electrophoretically deposited on ITO electrodes. Figure 18 shows a sharp *G* band at 1580 cm^{-1}, the so called *D′* band at 1609 cm^{-1} as a shoulder and the *D* band at 1311 cm^{-1}. Remarkably, the pyrrolidine-derivatized CNOs exhibit a strong band at 2618 cm^{-1}. No difference in the Raman spectra of the two pyrrolidine-derivatized products could be seen.

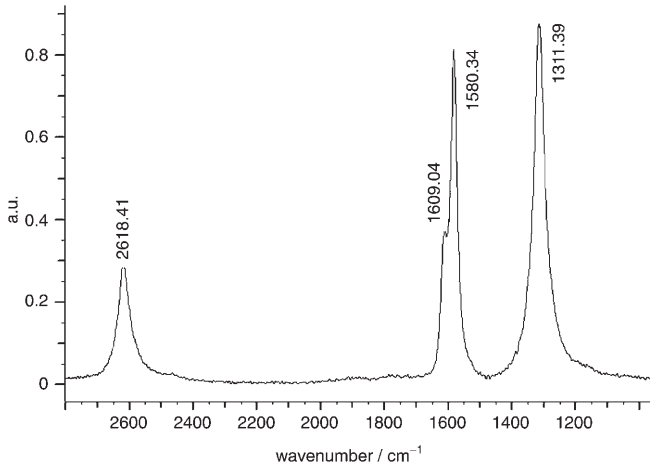

Figure 18. Raman spectra of pyrrolidine-derivatized CNO thin film (electrophoretically deposited on ITO electrodes).

Due to the small amount of sample NMR experiments including ^{13}C were not conducted so far (a ^{1}H NMR only shows two signals around 1 ppm).

Conclusion

Carbon nano-onions (CNOs) have been synthesized in preparative quantities using the graphite underwater arc discharge method. The raw CNO material thus obtained was collected, dried, and subsequently treated by thermal annealing, microwave heating, acid and supercritical water (SCW) washing. The purified CNOs were then functionalized utilizing several different synthetic reactions. Three reactions, namely PEGylation, amidation and 1,3-dipolar cycloaddition of CNOs, were carried out successfully; the amidation reaction also in a shorter time using a microwave reactor. Both the starting material and the functionalized products were characterized by transmission electron microscopy (TEM), thermal gravimetric analysis (TGA), Raman spectroscopy, and NMR spectroscopy. All functionalized CNO products were soluble in various organic solvents, and one synthesis produced water-soluble CNOs.

Experimental Section

Materials: All the chemicals were of analytical grade and used as received without further purification. Water was purified by a Milli-Q water purification system (Millipore) to a resistivity of 18.2 MΩ. The copper grids for TEM were bought from TED PELLA, Inc. (Prod. No. 01830, 200 mesh, Silicon Monoxide/formvar).

NMR spectroscopy: ^{1}H and ^{13}C NMR spectra were recorded on a Jeol Eclipse+500 spectrometer. Spectra were referenced to the residual proton resonance in $CDCl_3$ ($\delta = 7.26$ ppm, $\delta = 77.0$ ppm for ^{13}C) as the internal standard. Chemical shifts (δ) were reported as parts per million (ppm) on the δ scale downfield from TMS. Assignments were confirmed either by 2D NMR experiments or by means of NMR simulation software (ACD NMR predictor).

Transmission electron microscopy (TEM): The size and morphology of the products were observed by using a Hitachi Model HD2000 transmission electron microscope for high resolution images (HRTEM, 200 kV) and a Hitachi Model 7600 transmission electron microscope for low resolution images (LRTEM, 120 kV). The specimens under investigation were prepared from solution, dispersion, or embedded resin slices and deposited on copper grids.

Ultramicrotoming: For the preparation of 20 nm slices with an ultramicrotome (RMC PowerTome-XL), the sample under investigation was embedded in LR White Resin, a polar monomer polyhydroxylated aromatic acrylic resin. Less than 1 mg of compound was added to a vial filled with 1 mL of the resin. After curing the resin by heating overnight at 60 °C, thin slices were cut with self prepared glass knives (RMC glass knife maker) with the ultramicrotome (cutting speed 3 mm per s). The 20 nm thin slices were collected in a vessel filled with deionized water, subsequently deposited onto TEM copper grids, and dried in a desiccator overnight before TEM experiments.

Thermal gravimetric analysis (TGA) scan of PEGylated CNOs: TGA of the samples were conducted on a Mettler TGA/SDTA851. In a typical experiment, a functionalized CNO sample (18.5 mg) was loaded into an alumina pan under constant nitrogen flow (50 mL min^{-1}). The temperature ceiling was set at 500 °C, with a relatively slow scanning rate (5 °C min^{-1}) to ensure a complete thermal defunctionalization.

Raman spectroscopy: The Raman spectra were recorded using a Renishaw 1000 Raman spectrometer with the 785 nm emission line of a near infrared laser as the excitation source.

Electrophoretic deposition of modified and unmodified CNOs as films on electrode surfaces: The experimental details have been described else-

where by Kamat et al.[18] Tetraoctylammonium bromide (TOAB) was used to disperse non-soluble samples.

Synthesis and purification of the carbon nano-onions (CNOs): Graphite arcing experiments were conducted under deionized water (18.2 MΩ), as described in the literature,[11,48] using high purity graphite (POCO grade ZXF-5Q) for both the anode (0.25 inch) and cathode (1.0 inch). Despite the fact that arcing at different currents (20–70 A) seemed to give some control over the diameter of the CNOs produced, 30 A seemed to be the optimal choice, since running the arc discharge at lower currents resulted in very unstable arc discharges,[49] and higher currents gave rise to very exothermic and violent reaction conditions. The automated onion producing mechanism utilizing a DC gear motor and a variable output DC power supply and built in our lab for the synthesis of CNOs is shown in Figure 19. The power supply can be adjusted to drive the motor at the correct rate of speed to maintain an optimum distance between the electrodes for a constant-voltage arc, enabling a higher synthetic output rate than would be possible with only manual control.

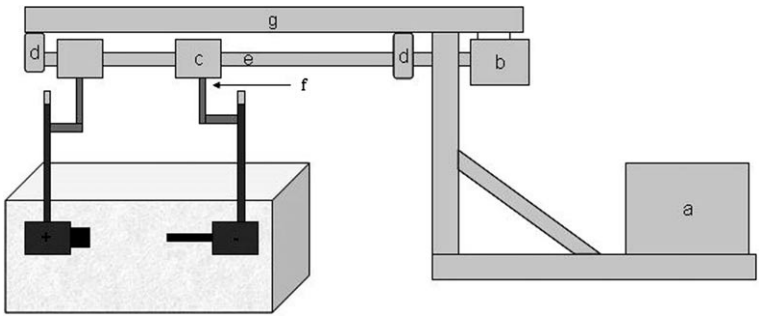

Figure 19. a) Variable output DC power supply; b) DC motor; c) guide bushing; d) threadless bolts; e) $^1/_4$ inch fine threaded steel rod; f) speedlock; g) aluminium frame.

Synthesis of PEGylated CNOs: In a typical experiment, an annealed (1 h, 400 °C) and nitric acid-treated sample (3 M, 48 h reflux) of CNOs (29.5 mg, 30 A, 17 V) was mixed with PEG_{1500N} (474 mg) and stirred for 19 d under argon in a round-bottom flask immersed in an oil bath heated to 140 °C.

After cooling to room temperature, deionized water (10 mL) was added to the flask and the resulting black-red suspension was sonicated for 5 min and transferred quantitatively to a SpectraPore membrane tubing (molecular weight cutoff ca. 12 kD) for dialysis against fresh deionized water for 76 h under vigorous stirring. The water surrounding the tubing was replaced every 24 h. After one day, the water had a light yellow color, but subsequent water portions remained colorless. After several centrifuging/decanting steps (until the supernatant aqueous solution remained colorless) and heat drying in the vacuum oven until the weight became constant, 17 mg of unreacted starting material was recovered. The dark-colored water solution of PEG_{1500N} functionalized CNOs was evaporated and after drying in the vacuum oven, 184 mg of a red brown viscous oil was obtained.

In order to eliminate unwanted side products, another dialysis was done (SpectraPore membrane tubing, molecular weight cutoff ca. 300 kD). After 24 h the outside water became yellow, but remained colorless thereafter. The remaining black solution inside the membrane was evaporated, dried and yielded 15% of the starting material as a black powder, which could be redissolved in water or any common organic solvent. The yellow solution outside the tubing was evaporated and yielded the remaining 85% as a red oil after drying in the vacuum oven.

Synthesis of octadecylated CNOs (solid-state reaction): In a typical reaction, 15.4 mg of the above-described purified CNOs (annealed and refluxed in HNO_3) and 1-octadecylamine ODA (50 mg) were placed together into a glass ampoule and evacuated to ca. 0.1 mbar, before the ampoule was sealed. The ampoule was placed in an oven preheated to 170 °C and baked there for 2 h. The ampoule was opened, put into a round bottom flask and the excess 1-octadecylamine was removed by evacuation of the flask with simultaneous heating at 170 °C. After cooling to room temperature, 10 mL of a 1:1 mixture of THF/$CHCl_3$ was added to the flask and the solution ultrasonicated for 1 h. After several cycles of centrifuging, decanting, adding of new solvent mixture to the black residue, ultrasonication etc., a dark black green transparent solution was obtained, which proved to be stable for months. The black residue, containing non-reacted and only partially derivatized CNOs, weighed 14.6 mg after drying in the vacuum oven (50 °C). The yield of the soluble part was 6.0 mg after evaporation of the solvent and drying in the vacuum oven (50 °C).

Synthesis of octadecylated CNOs (microwave reaction): In a typical experiment a mixture of annealed and acid treated CNOs (19.7 mg) was reacted with ODA (100 mg) and DMF (20 mL) in a 100 mL reaction Teflon chamber under microwave conditions (CEM Model 205 fitted with pressure and temperature controllers). After evaporating the DMF suspension, the excess ODA could be totally removed by heating the residue in vacuum (150 °C, 0.1 mbar). To the remaining 27.9 mg black powder, $CHCl_3$ (5 mL) was added and the solution sonicated for 4 h. The dark black green suspension was centrifuged for 2 h, the green transparent supernatant decanted, the black residue treated with another portion of fresh $CHCl_3$, and the whole procedure repeated until the supernatant remained colorless. Finally 11.5 mg of a black powder soluble in $CHCl_3$ (derivatized CNOs) and 16.4 mg of an unsoluble black residue (underivatized and partially derivatized CNOs) were obtained after drying in the vacuum oven (50 °C).

Pyrrolidine-derivatized CNOs: In a typical experiment, 4 mg of purified CNOs (annealed for 1 h at 400 °C, refluxed in 3 M HNO_3 for 48 h, annealed again for 1 h at 400 °C), *N*-ethylglycine (2 mg) and dodecanal (68 μL) were sonicated for 15 min in dry toluene (5 mL) and thereafter refluxed under argon for 4 d. After cooling to room temperature, centrifuging of the suspension yielded a black *solid 1* plus an orange *solution 1* (Figure 17). *Solid 1* was sonicated with toluene (5 mL) for 5 min. After centrifuging for 10 min, a slightly yellow clear toluene layer with black solid on the bottom was obtained. The toluene phase was added to *solution 1*. After a second addition of fresh toluene and another centrifuge cycle, a totally colorless toluene phase was obtained which again was added to *solution 1*. The vial with the collected toluene solutions was set aside (a TEM of this solution did not give any evidence of CNOs). Vacuum oven drying (50 °C) of *solid 1* afforded a black powder (4.7 mg), which was sonicated in $CHCl_3$ (5 mL) for 1 h. After centrifuging for 1 h, a deep black green *solution 2* was obtained with black solid on the bottom. After decanting *solution 2* and setting it aside, another portion of $CHCl_3$ (5 mL) was added, and the whole procedure repeated until the supernatant $CHCl_3$ solution remained colorless. All $CHCl_3$ solutions were collected, evaporated to dryness and vacuum dried at 50 °C, to afford a black *solid 3* (0.5 mg). The remaining, insoluble black *solid 2* weighed 4.2 mg after vacuum drying.

Following the same procedure as described above with the homologous aldehyde tridecanal under similar conditions (longer reaction time of additional 2.5 d) resulted in higher yields: starting from annealed CNOs (33.0 mg), a THF soluble black powder (18.6 mg) was obtained, as well as insoluble material (30.0 mg).

Acknowledgements

We thank the Chemistry Division of the National Science Foundation, grant CHE-0408367, for generous financial support.

[1] V. Georgakilas, D. M. Guldi, R. Signorini, R. Bozio, M. Prato, *J. Am. Chem. Soc.* **2003**, *125*, 14268.
[2] H. W. Kroto, J. R. Heath, S. C. O'Brien, R. F. Curl, R. E. Smalley, *Nature* **1985**, *318*, 162.
[3] S. Iijima, *Nature* **1991**, *354*, 56.
[4] D. Ugarte, *Nature* **1992**, *359*, 707.
[5] N. Sano, H. Wang, M. Chhowalla, I. Alexandrou, G. A. J. Amaratunga, *Nature* **2001**, *414*, 506.
[6] V. L. Kunetsov, A. L. Chuvilin, Y. V. Butenko, I. Y. Malkov, V. M. Titov, *Chem. Phys. Lett.* **1994**, *222*, 343.
[7] T. Cabioc'h, J. P. Riviere, J. Delafond, *J. Mater. Sci.* **1995**, *30*, 4787.
[8] X. H. Chen, G. T. Wu, F. M. Deng, J. X. Wang, H. S. Yang, M. Wang, X. N. Lu, J. C. Peng, W. Z. Li, *Wuli Xuebao* **2001**, *50*, 1264.
[9] a) B. S. Xu, S. I. Tanaka, *Nanostruct. Mater.* **1995**, *6*, 727; b) M. S. Zwanger, F. Banhart, A. Seeger, *J. Cryst. Growth* **1998**, *163*, 445.
[10] H. E. Troiani, A. Camacho-Bragado, V. Armendariz, J. L. Gardea Torresday, M. J. Yacaman, *Chem. Mater.* **2003**, *15*, 1029.
[11] a) V. Z. Mordkovich, A. G. Umnov, T. Inoshita, M. Endo, *Carbon* **1999**, *37*, 1855; b) V. Z. Mordkovich, *Chem. Mater.* **2000**, *12*, 2813.
[12] V. Z. Mordkovich, Y. Takeuchi, *Chem. Phys. Lett.* **2002**, *355*, 133.
[13] E. Koudoumas, O. Kokkinaki, M. Konstantaki, S. Couris, S. Korovin, P. Detkov, V. Kuznetsov, S. Pimenov, V. Pustovoi, *Chem. Phys. Lett.* **2002**, *357*, 336.
[14] N. Keller, N. I. Maksimova, V. V. Roddatis, M. Schur, G. Mestl, Y. V. Butenko, V. L. Kuznetsov, R. Schlögl, *Angew. Chem.* **2002**, *114*, 1962; *Angew. Chem. Int. Ed.* **2002**, *41*, 1885; .
[15] N. Sano, H. Wang, I. Alexandrou, M. Chhowalla, K. B. K. Teo, G. A. J. Amaratunga, *J. Appl. Phys.* **2002**, *92*, 2783.
[16] M. Chhowalla, H. Wang, N. Sano, K. B. K. Teo, S. B. Lee, G. A. J. Amaratunga, *Phys. Rev. Lett.* **2003**, *90*, 155504.
[17] S. Barazzouk, S. Hotchandani, K. Vinodgopal, P. V. Kamat, *J. Phys. Chem. B* **2004**, *108*, 17015.
[18] G. Girishkumar, K. Vinodgopal, Prashant V. Kamat, *J. Phys. Chem. B* **2004**, *108*, 19960.
[19] K. W. Street, M. Marchetti, R. L. Vander Wal, A. J. Tomasek, NASA report NASA/TM-2003–212301.
[20] A. Hirata, M. Igarashi, T. Kaito, *Tribol. Int.* **2004**, *37*, 899.
[21] D. Roy, M. Chhowalla, H, Wang, N. Sano, I. Alexandrou, T. W. Clyne, G. A. J. Amaratunga, *Chem. Phys. Lett.* **2003**, *373*, 52.
[22] Y.-P. Sun, K. Fu, Y. Lin, W. Huang, *Acc. Chem. Res.* **2002**, *35*, 1096.
[23] H. Hu, P. Bhowmik, B. Zhao, M. A. Hamon, M. E. Itkis, R. C. Haddon, *Chem. Phys. Lett.* **2001**, *345*, 25.
[24] D. B. Mawhinney, V. Naumenko, A. Kuznetsova, J. T. Yates Jr., J. Liu, R. E. Smalley, *Chem. Phys. Lett.* **2000**, *324*, 213.
[25] W. Huang, S. Fernando, L. F. Allard, Y.-P. Sun, *Nano Lett.* **2003**, *3*, 565.
[26] S. Tomita, T. Sakurai, H. Ohta, M. Fujii, S. Hayashi, *J. Chem. Phys.* **2001**, *114*, 7477.
[27] F. Tuinstra, J. L. Koenig, *J. Chem. Phys.* **1970**, *53*, 1126.
[28] D. S. Knight, W. B. White, *J. Mater. Res.* **1989**, *4*, 385.
[29] R. J. Nemanich, S. A. Solin, *Phys. Rev. B* **1979**, *20*, 392.
[30] H. Wilhelm, M. Leaurain, E. McRae, B. Humbert, *J. Appl. Phys.* **1998**, *84*, 6552.
[31] M. J. Matthews, M. A. Pimenta, G. Dresselhaus, M. S. Dresselhaus, M. Endo, *Phys. Rev. B* **1999**, *59*, R6585.
[32] A. M. Rao, A. Jorio, M. A. Pimenta, M. S. S. Dantas, R. Saito, G. Dresselhaus, M. S. Dresselhaus, *Phys. Rev. Lett.* **2000**, *84*, 1820.
[33] H. Hiura, T. W. Ebbsen, K. Tanigaki, H. Takahashi, *Chem. Phys. Lett.* **1993**, *202*, 509.
[34] E. V. Basiuk, M. Monroy-Pelaez, I. Puente-Lee, V. A. Basiuk, *Nano Lett.* **2004**, *4*, 863.
[35] V. A. Basiuk, K. Kobayashi, T. Kaneko, Y. Negishi, E. V. Basiuk, J.-M. Saniger-Blesa, *Nano Lett.* **2002**, *2*, 789.
[36] Y. Lian, Y. Maeda, T. Wakahara, T. Akasaka, S. Kazaoui, N. Minami, T. Shimizu, N. Choi, H. Tokumoto, *J. Phys. Chem. B* **2004**, *108*, 8848.
[37] M. Xu, Q. Huang, Q. Chen, P. Guo, Z. Sun, *Chem. Phys. Lett.* **2003**, *375*, 598.
[38] E. V. Basiuk, V. A. Basiuk, J.-G. Banuelos, J.-M. Saniger-Blesa, V. A. Pokrovskiy, T. Y. Gromovoy, A. V. Mischanchuk, B. G. Mischanchuk, *J. Phys. Chem. B* **2002**, *106*, 1588.
[39] Y. Song, A. S. Harper, R. W. Murray, *Langmuir* **2005**, *21*, 5492.
[40] R. L. Donkers, D. Lee, R. W. Murray, *Langmuir* **2004**, *20*, 1945.
[41] M. J. Hostetler, J. E. Wingate, C.-J. Zhong, J. E. Harris, R. W. Vachet, M. R. Clark, J. D. Londono, S. J. Green, J. J. Stokes, D. Wignall, G. L. Glish, M. D. Porter, N. D. Evans, R. W. Murray, *Langmuir* **1998**, *14*, 17.
[42] A. Badia, R. B. Lennox, L. Reven, *Acc. Chem. Res.* **2000**, *33*, 475.
[43] A. Badia, W. Gao, S. Singh, L. Demers, L. Guccia, L. Reven, *Langmuir* **1996**, *12*, 1262.
[44] Y. Wang, Z. Iqbal, S. Mitra, *Carbon* **2005**, *43*, 1015.
[45] M. Maggini, G. Scorrano, M. Prato, *J. Am. Chem. Soc.* **1993**, *115*, 9798.
[46] M. Prato, M. Maggini, *Acc. Chem. Res.* **1998**, *31*, 519.
[47] V. Georgakilas, K. Kordatos, M. Prato, D. M. Guldi, M. Holzinger, A. Hirsch, *J. Am. Chem. Soc.* **2002**, *124*, 760.
[48] F. Anariba, S. H. DuVall, R. L. McCreery, *Anal. Chem.* **2003**, *75*, 3837.
[49] S.-D. Wang, M.-H. Chang, J.-J. Cheng, H.-K. Chang, K. Ming-Der Lan, *Carbon* **2005**, *43*, 1322.

Received: May 9, 2005
Published online: September 28, 2005

